Atomic Resolution Three-Dimensional Electron Diffraction Microscopy

Jianwei Miao,[1,*] Tetsu Ohsuna,[2] Osamu Terasaki,[3] Keith O. Hodgson,[1,4] and Michael A. O'Keefe[5]

[1]*Stanford Synchrotron Radiation Laboratory, Stanford Linear Accelerator Center, Stanford University, Stanford, California 94309-0210*

[2]*Institute for Materials Research, Tohoku University, Sendai 980-8577, Japan*

[3]*Department of Physics and CIR, Tohoku University, Sendai 980-8577, Japan*

[4]*Department of Chemistry, Stanford University, Stanford, California 94305*

[5]*Materials Science Division, National Center for Electron Microscopy, Lawrence Berkeley National Laboratory, Berkeley, California 94720*

(Received 6 May 2002; published 18 September 2002)

We report the development of a novel form of diffraction-based 3D microscopy to overcome resolution barriers inherent in high-resolution electron microscopy and tomography. By combining coherent electron diffraction with the oversampling phasing method, we show that the 3D structure of a nanocrystal can be determined *ab initio* at a resolution of 1 Å from 29 simulated noisy diffraction patterns. This new form of microscopy can be used to image the 3D structures of nanocrystals and noncrystalline samples, with resolution limited only by the quality of sample diffraction.

DOI: 10.1103/PhysRevLett.89.155502 PACS numbers: 61.14.Dc, 61.14.Nm, 42.30.Rx

Electron lens aberration is the major barrier limiting the resolution of electron microscopy. The traditional approach to overcome the barrier is to use the holographic method, originally proposed by Gabor in 1948 [1]. Holography is a two-step imaging approach [2], including (i) obtaining a hologram from known reference waves and unknown object waves and (ii) converting the hologram to an image by using either light-optical or digital reconstruction. Recently, electron holography has been further developed to probe the local structures of crystals using photoelectron reference waves created from inside the sample itself [3,4]. Another approach has been to correct the electron microscope image for the effects of spherical aberration using a hardware corrector [5] or software reconstruction from images forming a focal series [6]. However spherically corrected images are still limited in resolution by chromatic aberration [7]. In this Letter, we describe a novel form of microscopy to overcome electron lens aberration (both spherical and chromatic). This form of microscopy does not require high-resolution electron lenses or reference waves and can image nanocrystals and noncrystalline samples in three dimensions at ultrahigh resolution.

When a beam of coherent electrons illuminates a finite sample, the electrons scattered by the Coulomb potential of the sample form a diffraction pattern in the far field. If the sample is thin enough that multiple scattering effects are negligible [8], the diffraction pattern is proportional to the square of the magnitude of the Fourier transform of the Coulomb potential. Because of the finite size of the sample, the diffraction pattern can be sampled at a spacing finer than the Nyquist frequency (i.e., the inverse of the size of the sample), which corresponds to surrounding the Coulomb potential of the sample with a region of zeros [9,10]. The finer the sampling frequency, the larger the region of zeros. When the region of zeros is larger than the Coulomb potential region, the phases are, in principle, available from the diffraction pattern itself and can be directly retrieved by using an iterative algorithm [11,12]. The first experimental demonstration of the oversampling method was carried out in 1999 by using soft x rays [13]. More recently, it has been applied to determine the 2D shapes of Au nanocrystals and the 3D structures of a noncrystalline nanostructured material using coherent hard x rays [14,15]. Application of the oversampling method to the electron diffraction has also been pursued to reconstruct a pair of fabricated holes in an opaque film at 5 nm resolution in two dimensions [16]. Here, we show that the combination of the coherent electron diffraction with the oversampling method can determine the 3D structures of nanocrystals and noncrystalline samples at atomic resolution.

Figure 1 shows the schematic layout of a 3D electron diffraction microscope. A beam of coherent electrons is generated by an electron gun and is focused to a small spot by a lens. An aperture is placed in front of the lens to adjust the spatial coherence. 3D electron diffraction microscopy requires high spatial and moderate temporal coherence, which are correlated to the oversampling degree approximately by

$$\alpha \leq \frac{\lambda}{4Oa} \quad \text{and} \quad \frac{E}{\Delta E} \geq \frac{2Oa}{d}, \tag{1}$$

with α the illumination semiangle shown in Fig. 1, λ the wavelength, $E/\Delta E$ the relative energy spread, d a desired resolution, O the oversampling degree which is equal to $\sqrt{\sigma}$ for a 2D sample with a size of $a \times a$ and $\sqrt[3]{\sigma}$ for a 3D sample with a size of $a \times a \times a$, and σ the oversampling ratio which is defined as the total volume of the Coulomb potential region and the region of zeros divided by the

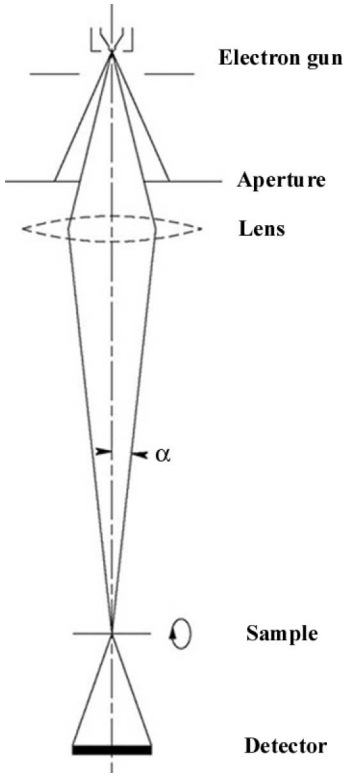

FIG. 1. Schematic layout of a 3D electron diffraction microscope.

volume of the Coulomb potential region. The sample, placed at the focal spot, can be rotated around a single axis for the 3D structure determination. A 2D area detector is placed downstream of the sample to obtain the oversampled diffraction patterns. Each component is in vacuum with a pressure comparable to that of transmission electron microscopy.

By using this form of microscopy with coherent electrons, we have carried out a computer simulation for the 3D structural determination of a nanocrystal (framework of Linde type A $[Al_{12}Si_{12}O_{48}]_8$) containing $2 \times 2 \times 2$ unit cells. This structure belongs to the cubic crystal system in space group $Fm\bar{3}c$, and the particle has a size of $49.22 \times 49.22 \times 49.22$ Å^3 [17]. Note that 3D diffraction microscopy cannot make use of the high symmetry of the structure since both the Bragg peaks and the intensity between these diffraction peaks are needed for structural determination. Figure 2(a) shows a section (0.5 Å thick) of the nanocrystal viewed along [100] at $z = 0$, in which the Coulomb potential of Si, Al, and O atoms was calculated by using a five-Gaussian approximation [18], and the Debye-Waller factors of Si, Al, and O atoms were set at 0.3, 0.3, and 0.5 Å^2, respectively. In the simulation, a beam of coherent electrons with an energy of 300 keV was used and the oversampling ratio (σ) was set at 4.3 in three dimensions. According to Eq. (1), the required spatial coherence of $\alpha \leq 6 \times 10^{-5}$ rad and the required temporal coherence of $E/\Delta E \geq 160$ were estimated for the studies, in which the temporal coherence can be easily satisfied since electron guns usually have $E/\Delta E \sim 10^5$. A limited parallel electron beam with coherence better than that required was simulated for the study, which is experimentally attainable by using the Koehler illumination condition. Since multiple scattering from the thin sample is negligible, the diffraction pattern is proportional to the square of the magnitude of the Fourier transform of the Coulomb potential.

By setting rotation angles from $-70°$ to $70°$ in $5°$ increments around a single rotation axis [19], a series of 29 2D diffraction patterns was calculated to a resolution of 1 Å. To make the computer simulation more realistic, noise was added to the diffraction patterns with a signal-to-noise ratio (SNR) of 3. To simulate a beam stop, an area of 11×11 pixels was removed from the center of each diffraction pattern, but the value of the center pixel in the diffraction pattern of the $0°$ projection was retained. We have found that the reconstructions are very sensitive to the value of the center pixel of the diffraction pattern, which is likely because the value of the center pixel represents the sum of the Coulomb potential. Figure 2(b) shows a diffraction pattern at the $0°$ projection, including both the Bragg peaks and the intensity between the Bragg peaks. The series of diffraction patterns was used to assemble a 3D magnitude of the Fourier transform with an array size of $160 \times 160 \times 160$ voxels. Because of the limited number of diffraction pattern projections, the assembled 3D magnitude included a number of undefined voxels whose initial values could not be calculated from the diffraction pattern projections.

The 3D magnitude can be directly converted to an image by using a 3D reconstruction algorithm without the need for interpolation. The algorithm first generated a 3D array of random phases. Combining the random phases and the 3D array of the known magnitude produced a new set of Fourier transform values. Applying an inverse Fourier transform to the 3D Fourier transform set, a 3D array of the Coulomb potential of the sample was obtained. Based on the oversampling ratio, a box of $54 \times 54 \times 54$ Å^3 was defined as the finite support, a boundary that is somewhat larger than the true envelope of the sample. Outside the finite support, the Coulomb potential was gradually pushed to zero. Inside the finite support, the negative Coulomb potential was pushed to zero and the positive Coulomb potential remained unchanged [20]. In this way, a new 3D array of the Coulomb potential was obtained. By applying the fast Fourier transform to the new 3D array, a new 3D Fourier transform was calculated. The magnitude of the new 3D Fourier transform was then replaced with the 3D array of the known magnitude, in which the value of those undefined voxels in the new 3D Fourier transform remained unchanged. This process represents one iteration of the algorithm.

After about 2000 iterations, the correct phases were retrieved, as indicated by an error function used for

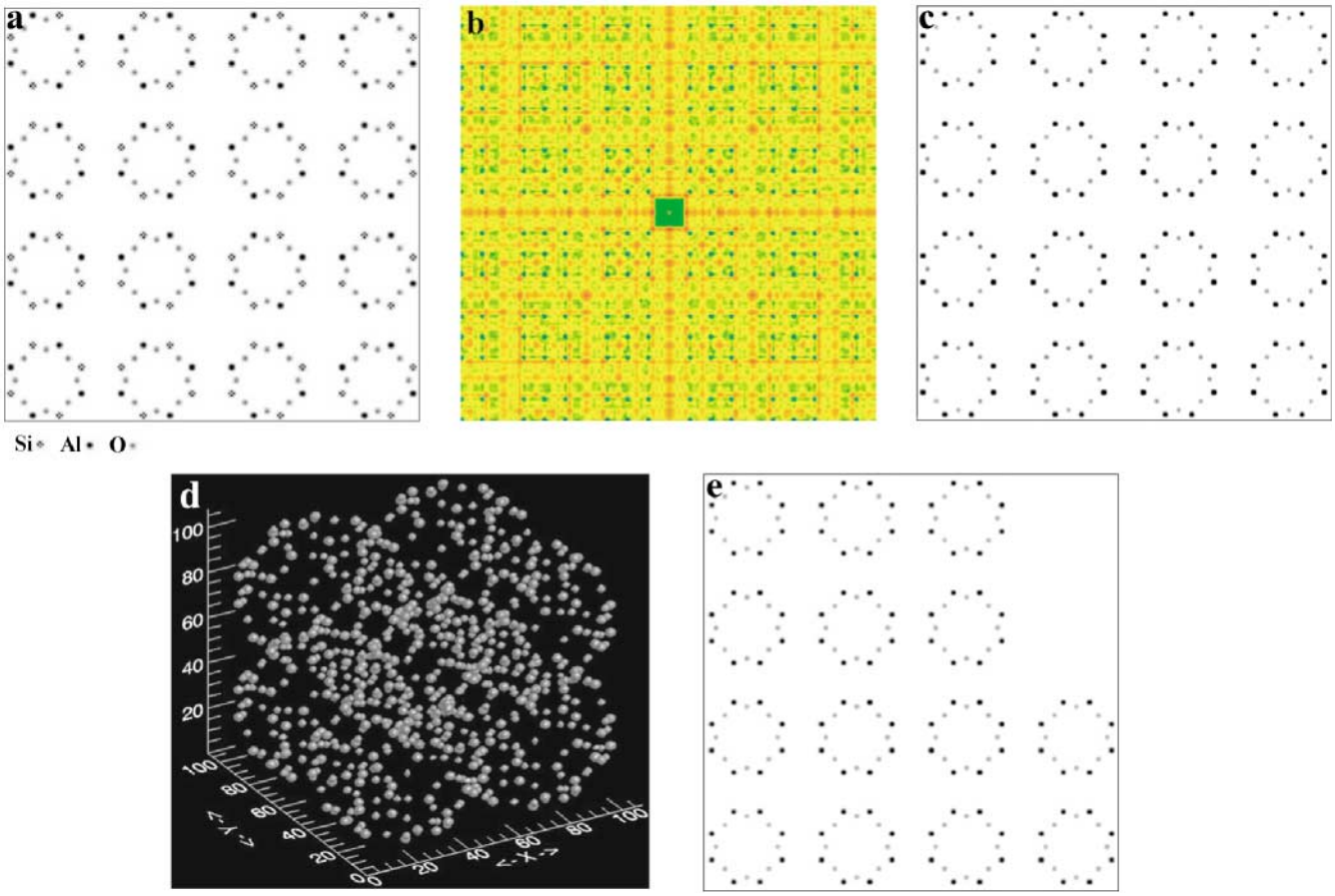

FIG. 2 (color). 3D structure determination of a $2 \times 2 \times 2$ unit cell nanocrystal (framework of Linde type A $[Al_{12}Si_{12}O_{48}]_8$) from a series of 29 diffraction pattern projections. (a) A section (0.5 Å thick) of the nanocrystal viewed along [100] at $z = 0$ with the image size of 49.22×49.22 Å^2. (b) The diffraction pattern (in a logarithmic scale) at the 0° projection in which the center square represents the missing data due to a simulated beam stop. The resolution at the edge corresponds to 1 Å. (c) The reconstructed section (0.5 Å thick) of the nanocrystal viewed along [100] at $z = 0$. (d) An iso-surface rendering of one-eighth of the reconstructed 3D Coulomb potential distribution (one unit cell) with the image size of $24.61 \times 24.61 \times 24.61$ Å^3. (e) The reconstructed section (0.5 Å thick) of the nanocrystal with defects viewed along [100] at $z = 0$.

monitoring the reconstruction [10]. Computation time for 2000 iterations on a 440 MHz Sun Solaris computing workstation is about 8 hours. Figure 2(c) shows a section (0.5 Å thick) of the reconstructed 3D Coulomb potential distribution viewed along [100] at $z = 0$, which is consistent with Fig. 2(a). Figure 2(d) shows an iso-surface rendering of one-eighth of the reconstructed Coulomb potential (one unit cell), in which the large spheres represent either the Al or Si atoms, and the smaller ones the O atoms. In Fig. 2(d), the pores and cages in the nanocrystal are also visible. Five more reconstructions were carried out by using different random phase sets as the initial input. The reconstructed Coulomb potential distribution was consistent among all six, which demonstrates the robustness of this approach.

Image reconstruction as a function of the SNR has also been studied. When the SNR was lower than 3, the quality of the reconstructed image deteriorated. To eliminate the effects of the symmetry and crystallinity on the image reconstruction, defects were created in the nanocrystal by removing part of the Coulomb potential at the upper-right corner. A series of 29 diffraction patterns with the SNR of 5 was generated from the nanocrystal with these defects, and the central 11×11 pixels were removed from each diffraction pattern except for the center pixel. By using the image reconstruction algorithm, the 3D structure of the nanocrystal with defects was successfully reconstructed, as shown in Fig. 2(e). While the simulated defects in the noncrystal is of special and ordered nature for demonstration purposes, the oversampling method can, in principle, handle samples with random defects [11] and grain boundaries.

By combining coherent electron diffraction with the oversampling method, we carried out a computer simulation to successfully determine the 3D structure of a nanocrystal (framework of Linde type A $[Al_{12}Si_{12}O_{48}]_8$) containing $2 \times 2 \times 2$ unit cells at a resolution of 1 Å. This form of microscopy can, in principle, be used to determine the 3D structure of nanocrystals and noncrystalline samples at ultrahigh resolution beyond the capability of

lens-based electron microscopy. In addition, the electron density necessary to record diffraction pattern is only about 10^{-2} of that required for high-resolution electron microscopy observation. Our experimental observation suggests that radiation damage may be related to electron density rather than electron dose. Compared with 3D electron crystallography, which reveals the averaged 3D structure of periodic objects [21,22], electron diffraction microscopy reveals the local nonaveraged 3D structure down to the single-atom level. Compared with electron tomography [23], this form of microscopy is less sensitive to sample movement and charging, does not require data interpolation, and easily bypasses the resolution limit due to sample thickness by considering each 2D diffraction pattern lying on the surface of the curved sphere (Ewald sphere) instead of a plane. We anticipate that 3D electron diffraction microscopy could have an important impact in the burgeoning field of nanoscience and technology for the 3D structure determination and characterization of nanoparticles.

We thank J. C. H. Spence for many stimulating discussions. The Stanford Synchrotron Radiation Laboratory is funded and operated by the U.S. Department of Energy, Office of Basic Energy Sciences with additional support provided by the Office of Biological and Environmental Research. The National Center for Electron Microscopy is funded by the Director, Office of Energy Research, Office of Basic Energy Sciences, Materials Science Division, and U.S. Department of Energy under Contract No. DE-AC03-76SF00098.

*Corresponding author.
Email address: miao@ssrl.slac.stanford.edu

[1] D. Gabor, Nature (London) **161**, 777 (1948).
[2] A. Tonomura, *Electron Holography*, Springer Series in Optical Sciences Vol. 70 (Springer, Berlin, Heidelberg, 1993).
[3] J. J. Barton, Phys. Rev. Lett. **61**, 1356 (1988).
[4] G. R. Harp, D. K. Saldin, and B. P. Toner, Phys. Rev. Lett. **65**, 1012 (1990).
[5] M. Haider, G. Braunshausen, and E. Schwan, Optik (Stuttgart) **99**, 167 (1995).
[6] W. M. J. Coene, A. Thust, M. Op de Beeck, and D. Van Dyck, Ultramicroscopy **64**, 109–135 (1996).
[7] M. A. O'Keefe, E. C. Nelson, Y. C. Wang, and A. Thust, Philos. Mag. B **81**, 1861–1878 (2001).
[8] While using a "thin sample" approximation in the Letter, we anticipate that a variety of nanomaterials can be studied by this form of microscopy. For light element, heavily faulted, and amorphous materials, sample thickness can range from a few tens of nanometer or thicker, depending on the energy of the electron beam. For perfect crystals of heavy elements, either thinner samples are desirable or the data collection with slight tilts (several millirad) away from zone axes is necessary to dramatically lower the degree of multiple scattering.
[9] D. Sayre, Acta Crystallogr. Sect. A **5**, 843 (1952).
[10] J. Miao, D. Sayre, and H. N. Chapman, J. Opt. Soc. Am. A **15**, 1662 (1998).
[11] J. Miao and D. Sayre, Acta Crystallogr. Sect. A **56**, 596 (2000).
[12] J. R. Fienup, Appl. Opt. **21**, 2758 (1982).
[13] J. Miao, P. Charalambous, J. Kirz, and D. Sayre, Nature (London) **400**, 342 (1999).
[14] I. K. Robinson, I. A. Vartanyants, G. J. Williams, M. A. Pfeifer, and J. A. Pitney, Phys. Rev. Lett. **87**, 195505 (2001).
[15] J. Miao, T. Ishikawa, B. Johnson, E. H. Anderson, B. Lai, and K. O. Hodgson, Phys. Rev. Lett. **89**, 088303 (2002).
[16] U. Weierstall, Q. Chen, J. C. H. Spence, M. R. Howells, M. Isaacson, and R. P. Panepucci, Ultramicroscopy **90**, 171 (2002).
[17] V. Gramlich and W. M. Meier, Z. Kristallogr. **133**, 134 (1971).
[18] L. M. Peng, G. Ren, S. L. Dudarev, and M. J. Whelan, Acta Crystallogr. Sect. A **52**, 257 (1996).
[19] We believe that the tilt increments required by this form of microscopy are related to the complexity of the sample structure and the desired resolution. In simulations, we have observed that the quality of the reconstructed structures gradually deteriorated as the rotation increments increased. These effects will be explored further in future studies.
[20] The imaging mechanism of 3D electron diffraction microscopy is somewhat different from that of transmission electron microscopy. The former reconstructs small phase shifts inside each resolution volume of the sample (a resolution volume is a sphere with the diameter corresponding to the resolution length), while the latter images the exit waves from the sample. Due to the small size of each resolution volume, a phase object for 3D electron diffraction microscopy is usually a weak phase object, which is not necessarily the case for transmission electron microscopy. In the computer simulation, we assumed that the absorption by the sample is negligible, which makes the small phase shifts inside each resolution volume not only linear proportional to the Coulomb potential but also real and positive. However, the oversampling phasing method works for the samples with complex Coulomb potential as well (see Ref. [10] for the computer simulation of the successful reconstruction of complex density distribution in x-ray diffraction using the oversampling phasing method).
[21] D. L. Dorset, Acta Crystallogr. Sect. A **54**, 750 (1998).
[22] K. H. Downing, M. Hu, H. Wenk, and M. A. O'Keefe, Nature (London) **348**, 525 (1990).
[23] J. Frank, *Electron Tomography* (Plenum, New York, 1992).